A fine actuation system control for the micro positioning parallel mechanism platform

Taewon Seo[1,#], Yongha Yoon[2], Hwasoo Kim[3], Deuksoo Kang[1] and Jongwon Kim[1]

1 School of Mechanical and Aerospace Engineering, Seoul National University, Seoul, South Korea
2 Wind power engineering team, Hyosung heavy industry, Seoul, South Korea
3Mechanical Engineering, Minnesota State University, Minnesota, USA
Corresponding Author / E-mail: seotw@rodel.snu.ac.kr, TEL: +82-2-880-7144, FAX: +82-2-875-4848

KEYWORDS : Precision control, Micro parallel mechanism, Physics-based modeling, System identification

This paper presents the feedback control of a fine actuation system in a micro positioning platform, which was recently developed to achieve the 3-DOF motions (x- and y-translations and α-tilting). First, a nonparametric model for the fine actuation system was built on the experimental data, which uncovers the underlying dynamics of the fine actuation system. Then, a physics-based model for the fine actuation system was developed through the constraint equations of the parallel mechanism and the dynamic equations of the fine actuation system. Based on the nonparametric model, physical parameters such as the mass, the stiffness and the damping were estimated to precisely predict the dynamics of the fine actuation system. Equipped with the physics-based model, the proportional and integral (PI)-based multi-input and single-output (MISO) controllers for the fine actuation system were designed to accomplish both high accuracy and fast response of the micro positioning platform. The decent performances of the synthesized controllers were successfully verified through the extensive experiments.

Manuscript received: August 15, 2007 / Accepted: 2007

NOMENCLATURE

$O\text{-}xyz$ = Fixed global reference frame
$O'\text{-}x'y'a'$ = Movable top frame
P_1, P_2, P_3 = Movable platform joints
B_1, B_2, B_3 = Base joints
b_1, b_2, b_3 = Vectices of base plate
L or (P_iB_i) = Length of link for each legs
R_1 or $(O'P_i)$ = Radius of moving platform
R_3 or (Ob_i) = Radius of base plate
Y_{C1}, Y_{C2}, Y_{C3} = Coarse actuator input displacements
X_{f1}, X_{f2}, X_{f3} = Fine actuator input displacements
m_1, m_2, m_3 = Masses of fine actuation part
c_1, c_2, c_3 = damping coefficients of fine actuation part
k_1, k_2, k_3 = stiffness coefficients of fine actuation part
F_1, F_2, F_3 = Generated force from fine actuators
V_1, V_2, V_3 = Input voltage to fine actuators
$\delta p, \delta q$ = Small displacements of input and output
J_q, J_p, J_f = Jacobian matrices of parallel mechanism

1. Introduction

Recently, it has become necessary to develop a micro factory that can manufacture and assemble micro-scale products since the commercial products are needed to have more functions in a small size. Most micro machining technologies are based on the semiconductor technology. However, to manufacture a complicate three dimensional product, the semiconductor technology has limitation because the technology is fundamentally based on two dimensional machining technologies. The traditional machining system is used to manufacture small three dimensional shaped products. But to manufacture small product, a larger system is loss of energy, space and time. So it is necessary to develop a small size manufacturing system.

Great attention has been given to parallel mechanism for some decades. Parallel mechanism has advantages in accuracy and speed. These two advantages are the most required functions to develop micro-scale positioning platform, so many have tried to adapt parallel mechanism to develop the positioning platform. Hasselbach et al. have investigated several positioning platforms based on parallel mechanism and emphasized the advantages of parallel mechanism in precision positioning field [1]. Yi et al. have designed and conducted experiment on the stiffness of the platform consisting of several flexure hinges [2]. Takeda et al. have designed parallel manipulator platform based on the Stewart-Gough platform using dual stage actuation system [3].

However, the above-mentioned parallel mechanism has limitation in rotational capability of below 20 degree. Low rotational capability is a representative disadvantage of parallel manipulators. To enhance the rotational capability of parallel mechanism, several researches have been performed. Liu et al. have suggested a family of 3-DOF parallel mechanism with high rotational capability of 100 degree [4]. And Kim et al. have suggested 6-DOF Eclipse-I and II mechanism which can rotate 90 and 360 degrees, respectively [5, 6]. The mechanism which is analyzed in this paper is suggested by Kang et al [7]. The rotational capability of the mechanism is 100 degree.

To enhance the accuracy and speed, controller design is a very important factor. For the parallel mechanism platforms, many control algorithms are applied and verified for accurate and fast motion.

Marquet et al. have simulated several kinds of control algorithm to the dynamic modeling of the parallel mechanism and have conducted experiment [8]. Karkoub et al. have designed a self tuner PID controller using neural network technique for the parallel mechanism which is applied to the haptic device [9]. Luo et al. have separated the dynamic model to slow time-scale and fast time-scale and have designed a separate controller based on the nonlinear control theory, and then they combined two kinds of controller into one main controller [10]. The parallel mechanism platform which is proposed by authors also needs to implement an adaptable controller to get fast and accurate response.

In Section 2, the developed micro parallel positioning platform is described. The mechanism is described and the problem is defined. Section 3 presents kinematic and dynamic modeling for controller synthesis. The unknown parameters are estimated by experiment. Section 4 presents the synthesis of controllers and results from simulation and experiment. Conclusion is suggested in Section 5.

2. Micro parallel positioning platform

2.1 Mechanism description

The micro parallel mechanism platform can realize 3-DOF motion. It can translate along the *x*- and *y*-axis and rotate for the *α*-axis (along the *x*-axis). The translational workspace is 5 mm X 5 mm and rotational workspace is 100 degree. The parallel mechanism is proposed in Fig. 1. The mechanism is composed of an end-effector, three links and base platform. The base platform and end-effector are connected by two identical links and one parallelogram shaped link. The parallelogram shaped link can confine the rotation of end-effector so the end-effector only can be rotated for the *α*-axis.

The actuation part consists of two sets of linear actuators: coarse and fine actuation. Coarse actuation part shows relatively long stroke and rough accuracy and fine actuation part shows relatively short stroke and fine accuracy. So the combination of these two kinds of actuation can realize long stroke and fine accuracy. The coarse actuation part was designed vertically to enhance the mobility of the mechanism and the fine actuation part was designed horizontally to increase the resolution of the mechanism.

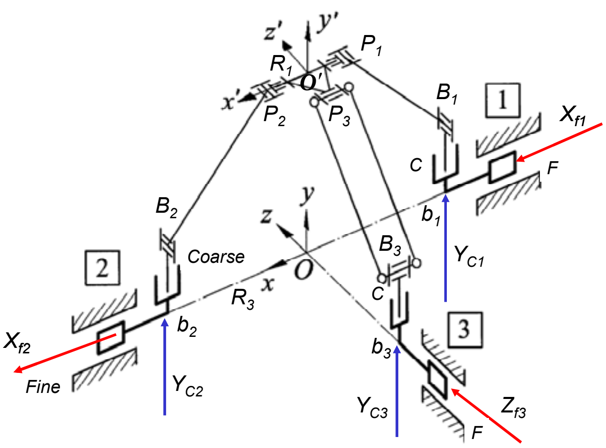

Fig. 1 3-DOF Parallel mechanism and actuation part

2.2 Manufacturing of the positioning platform

The micro positioning platform was manufactured and assembled. The overview of the platform is shown in Fig. 2. The total size of the platform is 280(w) X 200(d) X 408(h) mm. For low friction movement, six unique universal joints were used. The universal joint is presented in the right side of Fig. 2.

To enhance and measure the accuracy of the platform, a sensing part is required. To measure the 3-DOF motion of end-effector, three linear scales are attached to the end-effector. The sensing part is shown in the left side of Fig. 2.

At the bottom of Fig. 2, the tilting capability of the positioning platform is presented. Each photos show the tilting posture of the platform at -50, 0 and 50 degrees, respectively.

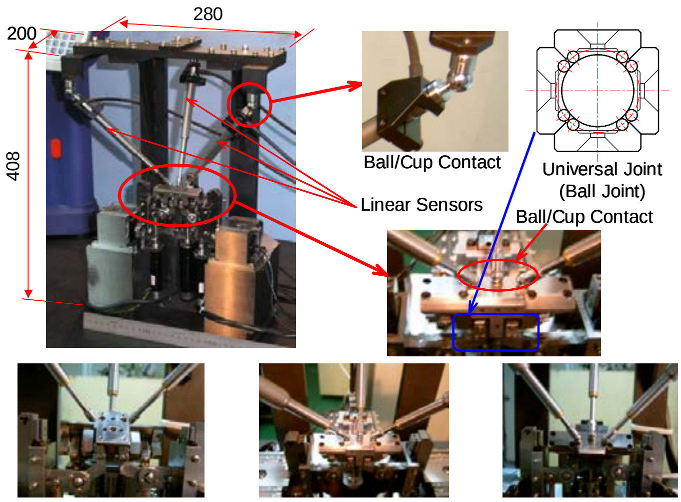

Fig. 2 Micro parallel positioning platform: Sensing part, universal joint and photos of rotation posture

2.3 Problem definition

In this paper, the modeling and control for the fine actuation part is presented. For accurate and fast movement of end-effector, fine actuation system control is very important. For the fine actuation part, linear PZT actuators were used, and the output of end-effector was measured by three linear scales.

3. Modeling of micro parallel positioning platform

3.1 Constraint equation

The kinematic constraint of the mechanism is that the length of each links is constant as shown in equation (1).

$$\| P_i - B_i \| = L \text{ , where } i = 1, 2, 3 \tag{1}$$

Three scalar equations can be generated from equation (1) for the three links, respectively, as follows:

$$(x - R_1 + R_3 - X_{f1})^2 + (y - Y_{c1})^2 = L^2 \tag{2}$$

$$(x + R_1 - R_3 - X_{f2})^2 + (y - Y_{c2})^2 = L^2 \tag{3}$$

$$(-R_1 \cos\alpha + R_3 - X_{f3})^2 + x^2 + (R_1 \sin\alpha + y - Y_{c3})^2 = L^2 \tag{4}$$

By using this constraints equation, the forward and inverse kinematics can be calculated.

3.2 Jacobian matrix

To formulate the dynamic equation, Jacobian matrix is required. Jacobian matrix is the relation of small perturbation of input and the response of output. By differentiating equations (2)-(4), we can get the equation in matrix form as follows:

$$J_p \delta p = J_q \delta q \tag{5}$$

where δp and δq represents $[\delta x \ \delta y \ \delta\alpha]^T$ and $[\delta X_{f1} \ \delta X_{f2} \ \delta X_{f3}]^T$, respectively. And J_p and J_q represent matrices as follows:

$$J_p = \begin{bmatrix} x - R_1 + R_3 - X_{f1} & y - Y_{c1} & 0 \\ x + R_1 - R_3 + X_{f2} & y - Y_{c2} & 0 \\ x & y + R_1 \sin\alpha - Y_{c3} & J_{x33} \end{bmatrix}$$

$$J_{p33} = (y + R_1 \sin\alpha - Y_{c3}) R_1 \cos\alpha + (-R_1 \cos\alpha + R_3 - X_{f3}) R_1 \sin\alpha$$

$$J_q = \begin{bmatrix} x - R_1 + R_3 - X_{f1} & 0 & 0 \\ 0 & x + R_1 - R_3 + X_{f2} & 0 \\ 0 & 0 & -R_1 \cos\alpha + R_3 - X_{f3} \end{bmatrix}$$

Then the Jacobian matrix of the fine actuation is defined as follows:

$$\delta p = J_f \delta q \text{, where } J_f = J_p^{-1} J_q . \tag{6}$$

3.3 Dynamic model

3.3.1 Dynamic formulation

The dynamic formulation is shown in Fig. 3. Each PZT actuators are assumed to be the mass-spring-damper system. The masses of links and end-effector are relatively lighter than the mass of each PZT actuation part, and so the masses were not included in the dynamic formulation. The dynamic equations for each PZT actuation parts are as follows:

$$F_i - k_i X_{fi} - c_i \dot{X}_{fi} = m_i \ddot{X}_{fi}. \qquad (7)$$

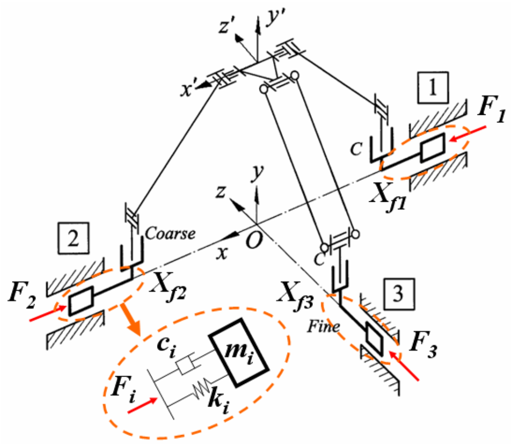

Fig. 3 Relation of force and dynamic response

By combining these independent dynamic equations and the Jacobian matrix (6) that represents the geometric constraints, we can get the state-space dynamic model of the micro parallel positioning platform as follows:

$$\begin{aligned}\dot{x} &= Ax + Bu \\ y &= Cx\end{aligned}, \quad x = [X_{f1}\ \dot{X}_{f1}\ X_{f2}\ \dot{X}_{f2}\ X_{f3}\ \dot{X}_{f3}]^{T} \qquad (8)$$

$$u = [F_1\ F_2\ F_3]^{T}, \quad y = [x\ y\ \alpha]^{T}$$

where

$$A = \begin{bmatrix} 0 & 1 & 0 & 0 & 0 & 0 \\ -\frac{k_1}{m_1} & -\frac{c_1}{m_1} & 0 & 0 & 0 & 0 \\ 0 & 0 & 0 & 1 & 0 & 0 \\ 0 & 0 & -\frac{k_2}{m_2} & -\frac{c_2}{m_2} & 0 & 0 \\ 0 & 0 & 0 & 0 & 0 & 1 \\ 0 & 0 & 0 & 0 & -\frac{k_3}{m_3} & -\frac{c_3}{m_3} \end{bmatrix}, B = \begin{bmatrix} 0 & 0 & 0 \\ \frac{1}{m_1} & 0 & 0 \\ 0 & 0 & 0 \\ 0 & \frac{1}{m_2} & 0 \\ 0 & 0 & 0 \\ 0 & 0 & \frac{1}{m_3} \end{bmatrix}$$

$$C = \begin{bmatrix} J_{f11} & 0 & J_{f12} & 0 & J_{f13} & 0 \\ J_{f21} & 0 & J_{f22} & 0 & J_{f23} & 0 \\ J_{f31} & 0 & J_{f32} & 0 & J_{f33} & 0 \end{bmatrix}$$

The relation of voltage to PZT actuators that is control input and the generated force from PZT that is input in the state-space model is verified by experiment as equation (9). Fig. 4 shows the experimental result between voltage and force of PZT.

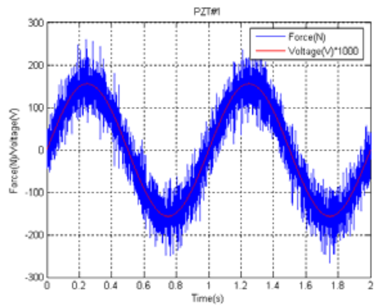

$$V_i = \frac{F_i}{1000} \qquad (9)$$

Fig. 4 Relation between input voltage and generated force

3.3.2 Parameter estimation

We set up the dynamic formulation of the micro parallel positioning platform, however, to apply this model to synthesize the controller, proper stiffness and damping coefficient are required. In this research, the parameters were identified by experiments.

The process is shown in Fig. 5. To ignore the nonlinear property like backlash, we did not use the white noise but sinusoidal inputs of several frequencies. Then we measured the magnitude change and phase delay of each sinusoidal input, and got the transfer relation which is indicated by a star, circle and diamond shaped points, respectively in Fig. 6.

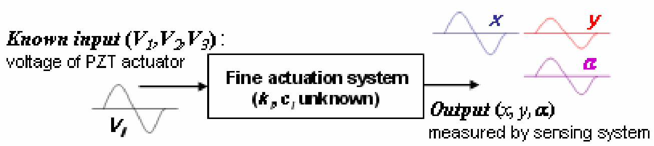

Fig. 5 Experimental process of parameter estimation

Then, we adjusted the damping and stiffness coefficient and checked the bode plot of the transfer matrix to match the state-space model and experimental result. To simplify the dynamic model, we assume that the mass, damping and stiffness coefficient are the same value in each link, respectively. The estimated mass, damping and stiffness coefficient are presented in Table 1.

Table 1 Estimated coefficient

Coefficient	m_i(kg)	c_i(N/μm·sec)	k_i(N/μm)
Value	0.804	0.00816	1.00

And the transfer matrix of the micro parallel positioning platform is shown in equation (10). And the frequency response of the model is shown as the solid lines in Fig. 6.

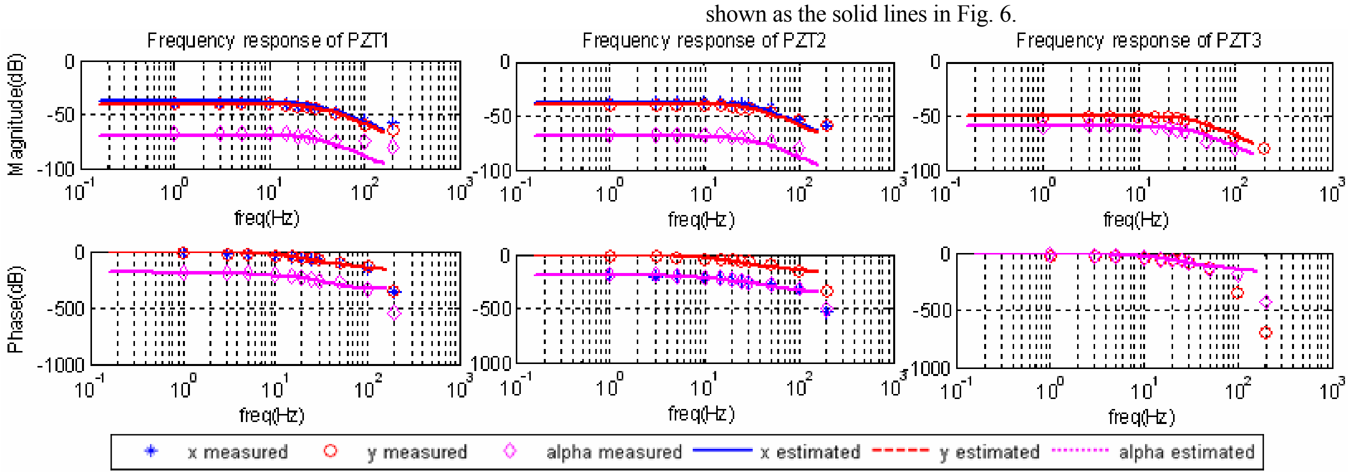

Fig. 6 Parameter estimation result and frequency response of estimated transfer matrix

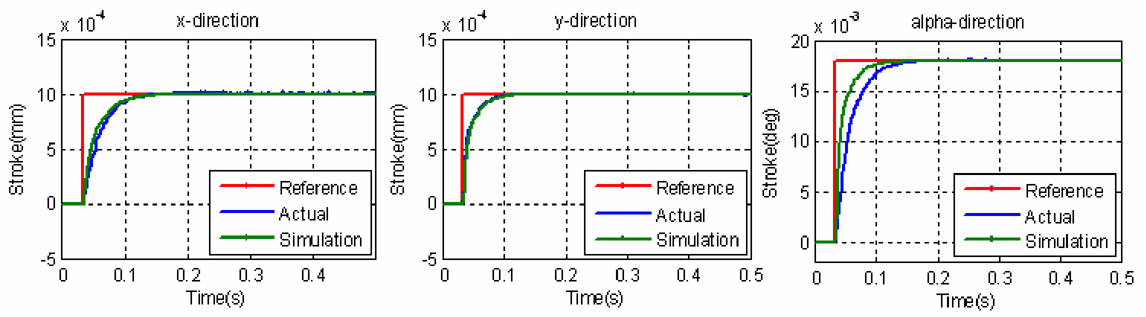

Fig. 7 Verification result of controller by simulation and experiment

The transfer matrix is composed of nine transfer functions. The transfer function from V_3 to x is assumed to be zero since the magnitude of the transfer function is relatively much lower than other transfer functions.

$$\begin{bmatrix} x \\ y \\ \alpha \end{bmatrix} = \begin{bmatrix} \frac{621.9}{s^2+406.1s+49750} & \frac{-621.9}{s^2+406.1s+49750} & 0 \\ \frac{510.4}{s^2+406.1s+49750} & \frac{510.4}{s^2+406.1s+49750} & \frac{161.7}{s^2+406.1s+49750} \\ \frac{-16.52}{s^2+406.1s+49750} & \frac{-16.52}{s^2+406.1s+49750} & \frac{50.05}{s^2+406.1s+49750} \end{bmatrix} \begin{bmatrix} V_1 \\ V_2 \\ V_3 \end{bmatrix} \quad (10)$$

4. Control of the fine actuation system

4.1 Objective for synthesis

The requirement of controller synthesis is summarized in Table 2. Each requirement is selected to design the micro positioning platform.

Table 2 Requirement of controller synthesis

Classification	Requirement
Steady-state error	< 0.05 μm
Overshoot	< 10%
Settling time	< 0.2 sec

4.2 PI-based MISO controller synthesis

Based on the transfer matrix in equation (10), we designed the PI-based controller for each transfer functions. The relation between proportional gain and integral gain was selected and then the proportional gain was designed to satisfy the requirement. As a design tool, the pole placement method was used to design the each controller. The synthesized controllers are as follows:

$$C(s) = \begin{bmatrix} \frac{18.0213(s+100)}{s} & \frac{18.0213(s+100)}{s} & 0 \\ \frac{21.9078(s+100)}{s} & \frac{21.9078(s+100)}{s} & \frac{70.1700(s+100)}{s} \\ \frac{686.8336(s+100)}{s} & \frac{686.8336(s+100)}{s} & \frac{228.5594(s+100)}{s} \end{bmatrix} \quad (11)$$

4.3 Result of simulation and experiment

The synthesized controller was verified through simulation and experiment. Step responses of the platform are shown in Fig. 7. There are no overshoot in each directional movement and steady-state errors are less than 0.02 μm. The settling times are 0.130, 0.130 and 0.140 sec in x-, y- and α-direction, respectively.

5. Conclusion

In this paper, we presented the dynamic modeling and controller synthesis for 3-DOF micro parallel positioning platform. As the geometric constraint, Jacobian matrix was calculated and as the dynamic relation, simple spring-damper model was calculated based on the assumption on fine actuation part. Based on the two results, state-space model was formulated. To estimate the damping and stiffness coefficient, experiment using sinusoidal input was performed. Based on the dynamic model, PI-based MISO controller was designed and the performance was verified through simulation and experiment. There were no overshoot in each directional movement and steady-state errors were less than 0.02 μm. And the settling times are 0.130, 0.130 and 0.140 sec in x-, y- and α-direction, respectively. Multi-input multi-output controller which also care the dynamics change along to the pose change is planning to be designed and verified. And dual servo controller is also planning to be developed.

ACKNOWLEDGEMENT

This work was sponsored by the Brain Korea 21 program and Engineering Research Center for Micro-thermal Systems.

REFERENCES

1. Hasselbach, J., Wreqe, J., Raatz, A., Becker, O., “Aspects on Design of High Precision Parallel Robots,” Assembly Automation, Vol. 24, No. 1, pp. 49-57, 2004.

2. Yi, B.J., Na, H.Y., Chung, G.B., Kim, W.K., Suh, I.H., “Design and Experiment of 3 DOF Parallel Micro-mechanism Utilizing Flexure Hinges,” Proceedings-IEEE International Conference on Robotics and Automation, Vol. 2, pp. 1167-1172, 2002.

3. Takeda, Y., Funabashi, H., Ichikawa, K., Hirose, K., “An In-parallel Actuated Manipulator with Redundant Actuators for Gross and Fine Motions,” Proceedings-IEEE International Conference on Robotics and Automation, Vol. 1, pp. 749-754, 2003.

4. Liu, X., Wang, J., Pitschow, G., “A New Family of Spatial 3-DoF Fully-parallel Manipulators with High Rotational Capability,” Mechanism and Machine Theory, Vol. 40, No. 4, pp. 475-494, 2005.

5. Kim, J., Park, F.C., Ryu, S.J., Kim, J.W., Hwang, J.C., Park, C.B., Iurascu, C., “Design and Analysis of a Redundantly Actuated Parallel Mechanism for Rapid Machining,” IEEE transaction on Robotics and Automation, Vol. 17, No. 4, pp. 423-434, 2001.

6. Kim, J., Hwang, J.C., Kim, J.S., Iurascu, C., Park, F.C., Cho, Y.M., “Eclipe-II: A new parallel mechanism enabling continuous 360-degree spinning plus three-axis translational motions,” IEEE transaction on Robotics and Automation, Vol. 18, No. 3, pp. 367-373, 2002.

7. Kang, D.S., Seo, T.W., Yoon, Y.H., Shin, B.S., Liu, X-J., Kim, J., “A Micro-positioning Parallel Mechanism Platform with 100-degree Tilting Capability,” Annals of the CIRP, Vol. 55, No. 1, pp. 377-380, 2006.

8. Marquet, F., Krut, S., Company, O., Pierrot, F., “ARCHI: A New Redundant Parallel Mechanism – Modeling, Control and First results,” IEEE International Conference on Intelligent Robots and Systems, Vol. 1, pp. 183-188, 2001.

9. Karkoub, M., Her, M.-G., Hsu, K.-S., Chen, C.-Y., “Neural-net Tuned PID Control of a Parallel Type Mechanism with Force Feedback for Virtual Reality Application,” Robotica, Vol. 22, No. 3, pp. 319-327, 2004.

10. Luo, L., Wang, S., Mo, J., Cai, J., “One the Modeling and Composite Control of Flexible Parallel Mechanism,” International Journal of Advanced Manufacturing Technology, Vol. 29, No. 7, pp. 786-793, 2006.